# THE DYNAMIC BEHAVIOR OF CASCADE PROCESSES –WITH APPLICATION TO DISTILLATION COLUMNS

John Morud and Sigurd Skogestad*
Chemical Engineering Dept., University of Trondheim-NTH
N-7034 Trondheim, Norway

Presented at the AIChE meeting, Miami Beach, Nov. 12-17, 1995.


Paper 189b

**Abstract**

The dynamic behavior of cascade processes is examined. By a cascade process, we here refer to an interconnected system consisting of many similar subsystems placed after one another, in such a way that a subsystem is influenced only by its nabor subsystems. An example of such a process is a distillation column, which is essentially a cascade interconnection of its individual trays.

By using Laplace transform techniques, we first show how the poles of simple cascades may be determined from the knowledge of the subsystem transfer functions. Knowing these pole locations, it is then straightforward to obtain, for example, a time response of the cascade. We then proceed to show how positive feedback interconnections of such cascade sections may result in very long time constants. Such long time constants have been observed in high purity distillation columns; in fact, the magnitude of these time constants may increase exponentially with the number of stages in the column. Another way of understanding this, apart from the transfer function point of view, is by analogy to diffusion in plug flow. We present such an analogy and illustrate the behavior of a simple binary distillation column from this point of view.

*Author to whom correspondence should be addressed. E-mail: skoge@kjemi.unit.no, Phone: 47-7359-4154, Fax: 47-7359-4080.

# 1 Introduction

Although most chemical processing plants consist of rather simple elements—such as flash tanks and pipes—their overall behavior can be rather complex, and very different from the behavior of the individual elements. An example is a distillation column, which is essentially a cascade interconnection of many simple flash tanks (trays). Even though the dynamic behavior of the individual elements—the trays—is easy to understand, it is not obvious without prior knowledge how the overall column behaves.

The purpose of this paper is to analyze the behavior of such cascaded processes. With a cascade we here refer to an interconnected system consisting of many similar subsystems placed after one another, in such a way that a subsystem is influenced only by its nabor subsystems. The obvious examples of cascades would be the countercurrent separation processes (such as distillation), or countercurrent heat exchangers. Many series connections of processing units also fall within this class, as the units in a series interconnection of processing units are often influenced by its *downstream* as well as its upstream neigbor. For example, the flow rate from a unit is often influenced by the pressure in the downstream unit.

We emphasize that it is not our purpose to develop accurate models for computer simulation of cascade processes. Such simulation models are well established, and it is straightforward to do numerical simulations of, for instant, a distillation column. Our main purpose is qualitative insight into cascade behavior.

The paper may be thought of as consisting of two parts. In the first part, we treat cascades from a general point of view, using Laplace transform techniques. We first define what we mean with a cascade, and give an expression for the pole locations of cascades consisting of identical scalar subsystems. We then specialize on conservative systems, which typically arise from conservation equations for mass and energy. We proceed by giving several examples, i.e. by analyzing the concentration dynamics of a stripping column; the pressure dynamics of a train of vessels; and the dynamics of heat conduction in plug flow.

In the second part of the paper, we analyze in more detail a binary distillation column. We first do some numerical experiments to show that the slow time constant of the column depends exponentially on the number of equilibrium stages. We then propose a simple conceptual model of the column in order to shed some light on this exponential dependence. Finally, we apply concepts from the simple model to the binary distillation column to illustrate the column behavior.

The rest of this introduction is devoted to reviewing previous work.

Lapidus and Amundson (1950) consider the transient behavior of adsorbsion and extraction equipment. By analytical treatment, they solve simple models of such columns, and find expressions for the step responses. Their treatment is rather involved, but contains many insights.

Montroll and Newell (1952) approximate multistaged cascade processes by nonlinear partial differential equations, and find analytical solutions for such equations.

Rosenbrock (1960) discuss a "conservation property" of distillation columns. He shows how a particular measure of deviation from steady state operation may be thought of as a "conserved" property in the column.

Rosenbrock (1962) reviews previous work on the transient behavior of distillation columns and heat exchangers. He discusses approximation of distillation column models by means of partial differential equations.

Williams (1963) reviews the status of results on the dynamic behavior of mass transfer processes at that time (1963), and lists some problems that require further investigation (per 1963).

Haagensen and Lees (1966) compare experimental frequency responses with theoretical models for a gas absorbtion column, and obtain fair agreement between the experiments and their model. The theoretical model consists of simple transfer function models derived from mass and energy balances.

Levy *et. al.* (1969) perform modal decompositions of some models for binary distillation. They conclude that the composition dynamics is much slower than the hydraulics, which means that these phenomena tend to be decoupled; that is, the hydraulics may be considered quasi-stationary compared to the composition dynamics.

Osborne (1971) develops approximate models for multicomponent distillation columns by using partial differential equations. Simulations indicate that his approach yields accurate results.

Kim and Friedly (1974) study countercurrent cascades of equilibrium stages, and develop simple low-order-plus-delay transfer functions for such cascades. They refer to Lapidus and Amundson (1950) as being the first to obtain analytical expressions for the eigenvalues of countercurrent cascades.

Wong and Luus (1980) consider model reduction of multistage systems by means of orthogonal collocation. They obtain good agreement between step responses of their reduced order models with the original high order models.

Cho and Joseph (1983) use partial differential equations approximations of separation processes together with orthogonal collocation in order to obtain reduced order models of such processes.

Fuentes and Luyben (1983) consider control of high-purity distillation columns. By computer simulations of columns, they show that such columns may be controlled effectively despite the large linearized time constants of high-purity distillation columns.

Celebi and Chimowitz (1985) continue the work by Kim and Friedly, and derive simple second-order-plus-delay transfer functions for cascades.

Kapoor and McAvoy (1986a) study the effect of distillation column recycle structure on distillation column

time constants, and present a method for estimating time constants of such columns.

Kapoor and McAvoy (1986b) present analytical expressions for predicting distillate and bottoms composition transient responses for distillation columns.

Skogestad and Morari (1987) develop simple transfer function models for binary distillation columns, and find simple expressions for the dominant time constant of such columns. For high purity columns, they found excellent agreement between the simple expressions and detailed calculation.

Of other related work, we mention Marquardt (1990), Hwang (1990 and 1991), Tabrizi (1990) and Kienle and Marquardt (1992).

# 2 Cascade interconnections

Most of this paper is specialized to a simple type of cascades, namely scalar cascades consisting of identical subsystems. However, we will first present what we mean by a cascade *in general*.

## 2.1 Distinctions and definitions

We distinguish between cascades with **identical** and **nonidentical** subsystems and between **linear** and **nonlinear** cascades.

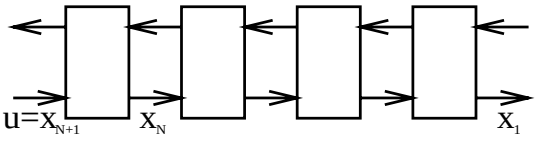


Figure 1: General cascade interconnection

### Nonlinear cascades

By a **cascade**, we mean a system of N similar subsystems placed after one another, such that the state of subsystem $j$ is determined by the subsystem preceding and following that subsystem (see Fig. 1). Formally, we may write $x_j = \mathcal{N}_j(x_{j+1}, x_{j-1})$, where $x_j$ is a vector that determines the state of subsystem $j$ ($j = 1, 2, \cdots, N$), and $\mathcal{N}_j$ is an (in general nonlinear) operator. This definition is fairly general—perhaps too general to yield much insight into cascade behavior. For insight, it is thus convenient to study linear cascades.

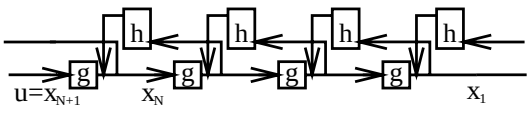


Figure 2: Linear cascade interconnection

### Linear cascades

By a **linear** cascade, we mean a system on the form:

$$x_j(s) = G_j(s)x_{j+1}(s) + H_j(s)x_{j-1}(s) \qquad (1)$$

Here, $G_j$ and $H_j$ are transfer matrixes. This interconnection structure is shown in Fig 2. A special case applies to scalar systems, in which case we will use lower case letters, $g_j$ and $h_j$. In the case where $g_j$ and $h_j$ are the same for all stages, we drop the subscript $j$.

## 2.2 Some theoretical results

It is straightforward to do numerical simulations of such systems, even in the nonlinear case. For example, one may use a standard state space model. However, there are other computational forms, which may be convenient for analytical purposes. The aim of the present section is to find analytical expressions for the pole and zero locations of scalar cascades.

### A recursion formula

Consider a linear cascade with N stages—described by eq. 1. Suppose that we want to find the overall transfer function, say $T_N$, between $u$ ($\equiv x_{N+1}$) and $x_1$ (see Fig. 2). To do this, consider factorizing $T_N$ into

$$T_N = \Pi_{j=1}^{N} S_j \qquad (2)$$

where $S_j$ is the transfer function between two consecutive stages, $x_j = S_j x_{j+1}$. By inserting this expression into equation 1 and collecting terms, one obtains the following recursion formula for $S_j$:

$$S_j = (I - H_j S_{j-1})^{-1} G_j, \quad S_0 = 0, \quad j = 1, 2 \cdots N \qquad (3)$$

Note that the transfer function $S_0$ is a fictitious quantity; the meaningful $S_j$'s start with $j = 1$.

### Structure of the overall transfer function.

The advantage of the recursion formula above, is that it makes it possible to analyze analytically the connection between the behavior of the subsystems and the behavior of the overall system. For scalar linear systems of identical subsystems,

$$x_j(s) = g(s)x_{j+1}(s) + h(s)x_{j-1}(s) \quad , \qquad (4)$$

the overall transfer function, $T_N$, may thus be factored into (Derived in Appendix A):

$$T_N(s) = \frac{g(s)^N}{\Pi_n(1 - k_n g(s)h(s))} \qquad (5)$$

where:

$$k_n = 4\cos^2\left(\frac{n\pi}{N+1}\right), \quad n = 1, 2, \cdots \left\lfloor \frac{N+1}{2} \right\rfloor \qquad (6)$$

This expression provides a generalization of results of previous authors (e.g. Celebi and Chimowitz 1985; Kim and Friedly 1974; Lapidus and Amundson 1950). The relevance of achieving a factorized expression for $T_N$, is that this makes the relation between the subsystems and the overall system transparent.

This means that the pole (and zero) locations of the overall system, $T_N$, may be inferred directly from the subsystem transfer functions, $g$ and $h$. The pole locations are important, as they determine the stability and speed of response of the system, and thus essentially determine its dynamic behavior.

Note that the zeros of the denominator, $\Pi_n(1 - k_n g(s)h(s))$, all lie on the root locus of $L \equiv gh$, with feedback gains as given by the $k_n$'s (equation 6). For simple systems, the root locus of $gh$ may easily be sketched by hand. It is thus easy to predict qualitatively the pole locations of scalar cascades of identical subsystems, and thus their dynamic behavior.

Before we turn to some specific examples of cascades, we specialize the results of this section (eqs. 4 and 5) to conservative systems.

### 2.3 Special case: First order conservative systems

In many instances, differential equations arise from conservation equations for mass or energy. This restricts the possible behavior significantly.

Here, we specialize on a restricted class of cascades, described by first order constant coefficient linear equations on the form ($b_j$ is assumed negative):

$$\frac{d(M_j x_j)}{dt} = a_j x_{j-1} + b_j x_j + c_j x_{j+1} \tag{7}$$

This equation is hereafter denoted as **conservative** if the following sum of coefficients is zero:

$$a_{j+1} + b_j + c_{j-1} = 0 \tag{8}$$

The reason for this definition is seen if we look at the change in the sum of the variable $M_j x_j$ over several stages ($m > n$):

$$\frac{d}{dt}(\sum_{j=n}^{j=m} M_j x_j) = \sum_{j=n}^{j=m} \frac{d}{dt}(M_j x_j) =$$

$$a_n x_{n-1} + (a_{n+1} + b_n)x_n + (b_m + c_{m-1})x_m + c_m x_{m+1} \tag{9}$$

It is seen that terms cancel, in such a way that only terms at the summation limits, $m$ and $n$, remain. The interpretation is that an increase (decrease) of $Mx$ at one stage implies a similar decrease (increase) in the neighboring stages. For example, this would be the case if $x$ is a conserved quantity which is transported from one subsystem to its neighbor.

**Poles of conservative cascades**

We analyze in more detail the case when the coefficients, $a$, $b$ and $c$, are identical for all stages, and $M_j = M = 1$. Taking Laplace transforms and collecting terms, one obtains:

$$x_j = \frac{1-\beta}{1+\tau s} x_{j+1} + \frac{\beta}{1+\tau s} x_{j-1} \tag{10}$$

where $\beta = \frac{a}{a+c}$ and $\tau = \frac{1}{a+c}$.

This is on the standard form, eq. 4, with

$$g = \frac{1-\beta}{1+\tau s} \quad and \quad h = \frac{\beta}{1+\tau s} \tag{11}$$

The poles of the cascade may therefore be found analytically by solving the characteristic equation $1 - k_n g(s)h(s) = 0$ for $s$, which yields (The $k_n$'s are given by eq. 6):

$$s = \frac{1}{\tau}[-1 \pm 2\sqrt{\beta(1-\beta)}\cos(\frac{n\pi}{N+1})] \tag{12}$$

Similar expressions have been obtained by previous authors (e.g. Celebi and Chimowitz 1985; Kim and Friedly 1974; Lapidus and Amundson 1950).

We distinguish between the following two cases:

1. $\beta \in < 0, 1 >$. In this case, the poles are negative real (i.e. in the Left Half Plane).

2. $\beta \notin < 0, 1 >$. In this case, the poles are complex conjugates in the Left Half Plane.

The slowest time constant—corresponding to a pole close to zero—occurs when $\beta = 1/2$. To see this, introduce the approximation $\cos x \approx 1 - x^2/2$ into eq. 12, which applies when $x$ is small, i.e. when $N$ is large. The slowest pole then becomes (for $n = 1$):

$$s \approx -\frac{1}{2\tau}(\frac{\pi}{N+1})^2 \tag{13}$$

Hence, the time constant may increase proportionally with the *square* of the number of stages (relative to the time constant of a single stage), which is a well known result (Lapidus and Amundson, 1950). However, if $\beta$ is not exactly equal to 1/2, then as $N \to \infty$, the slow pole approaches

$$s = \frac{1}{\tau}[-1 + 2\sqrt{\beta(1-\beta)}] \tag{14}$$

That is, the slow pole approaches a fixed value. Hence, the time constant is asymptotically **independent** of the number of stages if $\beta \neq 1/2$.

Note that all this applies to an **open ended** column section. As will be shown below, the slowest time constant may increase **exponentially** with $N$ when two linear cascades are interconnected.

### 2.4 Time constants of interconnected cascades

In this section, we explain why the interconnection of two linear cascades may result in very long time constants. In order to keep the essential ideas, and not drown in details, we will simplify the arguments; hence, we do not **prove** any results. The arguments are similar to those of Kapoor and McAvoy (1986).

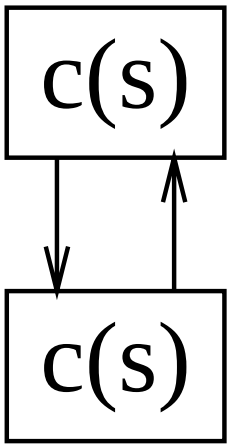


Figure 3: Feedback interconnection of cascades

Consider the feedback interconnection of two transfer functions, $c(s)$, as shown in Fig. 3. Each of the two transfer functions may be thought of as representing a column section in, for instant, a distillation column. We assume that the transfer function $c(s)$ is rational, with a gain **very close to one**, i.e. with a transfer function on the form:

$$c(s) = (1-\epsilon)\frac{\Pi_{zeros}(1+\tau_z s)}{\Pi_{poles}(1+\tau_p s)} \tag{15}$$

Close to the origin of the complex plane, this transfer function may be approximated as a first order transfer function:

$$c(s) \approx \frac{1-\epsilon}{1+\tau s} + O(s^2) \quad where \quad \tau = \sum_{poles}\tau_p - \sum_{zeros}\tau_z \tag{16}$$

To find the closed loop poles, we form the return difference:

$$0 = 1 - c(s)^2 = [1+c(s)][1-c(s)] \tag{17}$$

Consider the last factor, $1-c(s)=0$. Inserting the simplified transfer function, eq. 16, and solving for $s$ yields:

$$s = -\epsilon/\tau \tag{18}$$

Hence, the slowest time constant has been magnified by a factor $1/\epsilon$ compared to the individual transfer functions, and if $\epsilon$ is sufficiently small, the closed loop time constant will be very large. This is seen to be an effect of **positive feedback** between the two transfer functions.

As shown by Kapoor *et al.*, the corresponding feedback gains in a high purity distillation column is indeed close to one. To see this, think of the following thought experiment:

Consider tearing a distillation column into two equal parts, each part represented by the transfer function $c(s)$; then consider the lower of the two parts. Imagine that we may somehow manipulate the composition in the liquid stream into this part. We look at the gain from molar flow rate of light component in this liquid stream to the molar flow rate of light component in the vapor stream at the same position. Obviously, this is very close to one for a high purity distillation column, since almost all light component is returned in the vapor stream. In other words, an increase in the molar flow rate of light component at steady state results in an almost equal increase of the molar flow rate of this component in the vapor stream.

We turn to some specific examples of cascade interconnections.

### 2.5 Examples of cascade interconnections

The purpose of the examples below, is to illustrate the application of the above results, and to draw the attention to similarities between different physical systems. These similarities make it possible to use the examples as analogies for each other, thus enhancing the understanding of each of them individually. Such an analogy is exploited in a later section when analyzing binary distillation.

#### Example 1. Concentration dynamics of a stripping or adsorbtion column

Consider the concentration dynamics of a section in a stripping or absorbtion column. It is assumed that the equilibrium line is linear in the range of compositions in the section. As a simple model, take:

$$M\frac{dx_j}{dt} = L(x_{j-1}-x_j) + V(y_{j+1}-y_j); \quad y_j = Kx_j \tag{19}$$

where $M$ is the molar holdup on each stage; $L$ and $V$ are the liquid and vapor molar flow rates; and $x$ and $y$ are the liquid and vapor mole fractions of light component.

Taking the Laplace transform and collecting terms we obtain:

$$x_j = \frac{1-\beta}{1+\tau s}x_{j+1} + \frac{\beta}{1+\tau s}x_{j-1} \tag{20}$$

where $\beta = \frac{1}{1+\frac{VK}{L}}$ and $\tau = \frac{M}{L+VK}$. The quantity $\tau$ may be interpreted as the time constant of a single tray, whereas the gain $\beta$ is a function of $\frac{VK}{L}$–the ratio between the slopes of the equilibrium- and the operating line in a McCabe-Thiele diagram. As the equation is identical to eq. 10, all arguments following that equation apply. Specifically:

1. The eigenvalues (poles) are all real in this case, since $\beta \in < 0, 1 >$.

2. The slowest eigenvalue–which is the one closest to zero–is found for $n = 1$, $\beta = 1/2$ in eq. 12 ($s = \frac{1}{\tau}[-1 + \cos(\frac{\pi}{N+1})]$ ). This corresponds to parallel equilibrium- and operating lines in a McCabe-Thiele diagram. According to the approximation above, eq. 13, the time constant may then be proportional to $N^2$, the square of the number of stages. In practice, these large time constants are strongly reduced if $\beta$ is not exactly equal to 1/2. The next slowest eigenvalue is found for $n = 2$ ($s = \frac{1}{\tau}[-1 + \cos(\frac{2\pi}{N+1})]$ ) and is approximately a factor *four* faster than the slowest one. Again, this only applies in the special case $\beta = 1/2$.

**Example 2. Pressure dynamics of a train of vessels**

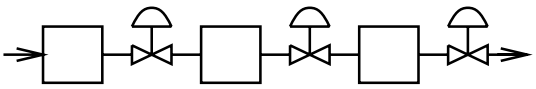

Figure 4: Pressure vessels in series

Consider the pressure dynamics of a train of vessels, as depicted in Fig 4. The pressure is specified at both sides. This has sometimes been proposed as a conceptual model of the vapor dynamics of distillation columns (e.g. Rademaker *et. al*, 1975). Inertia effects are assumed negligible, and the pressure drop between the vessels is assumed to be proportional to the square of the volume flow rate, and the same for all vessels. A simple model for the system may then be written as an equation for the pressure, $p_j$ (deviation variable), in vessel $j$ (derived in Appendix B):

$$2\tau\frac{dp_j}{dt} = p_{j+1} - 2p_j + p_{j-1} \tag{21}$$

Here, the time constant of a single vessel, $\tau = \frac{\Delta p}{nP}\cdot\tau_{res}$, is a function of the pressure drop between vessels, $\Delta p$; the absolute pressure in the vessels, $P$; the polytropic coefficient, $n$; and the vessel residence time, $\tau_{res}$.

The model may be written in the standard form as:

$$p_j = \frac{1/2}{1+\tau s}p_{j+1} + \frac{1/2}{1+\tau s}p_{j-1} \tag{22}$$

so

$$g(s) = h(s) = \frac{1/2}{1+\tau s} \tag{23}$$

which is a special case of eq. 10 with $\beta = 1/2$.

**Example 3. A distributed parameter system: Heat conduction in plug flow**

Consider plug flow of a conducting fluid in an insulated pipe. The temperature, $T$, of the fluid is governed by the equation:

$$\frac{\partial T}{\partial t} + u\frac{\partial T}{\partial z} = \nu\frac{\partial^2 T}{\partial z^2} \tag{24}$$

where $u$ and $\nu$ are the fluid velocity and thermal diffusivity; and $z$ is the position in the pipe.

The purpose of presenting this example is threefold: First, to exemplify the application of the above results on a distributed parameter system; second, to show how the stability of finite difference schemes for numerical calculations may be analyzed in this framework; and third, to provide a physical analogy for the other examples. This analogy will be exploited in a later section.

By discretizing using central differences with $h = L/N$ this becomes:

$$\frac{dT_j}{dt} + u\frac{T_{j+1} - T_{j-1}}{2h} = \nu\frac{T_{j+1} - 2T_j + T_{j-1}}{h^2} \tag{25}$$

which may be recast into the standard form by taking Laplace transforms and collecting terms:

$$T_j = \frac{1/2 - Pe/4}{1+\tau s}T_{j+1} + \frac{1/2 + Pe/4}{1+\tau s}T_{j-1} \tag{26}$$

where $Pe = \frac{uh}{\nu}$ is a Peclet number and $\tau = \frac{h^2}{2\nu}$ is a (conduction) time constant.

This is again a special case of eq. 10 with $\beta = 1/2 + Pe/4$. In this case the parameter $\beta$ is not bounded between zero and one, which means that we may get complex conjugate poles for values of $\beta$ outside this range, i.e. for $|Pe| > 2$.

It is well known that one may get numerical difficulties applying central differences in this example when $|Pe| > 2$. This is seen to be caused by very lightly damped complex conjugate poles introduced by the discretization scheme. Integration of this system would therefore be rather difficult by most higher order numerical methods, and it's stability might depend on the way the boundary conditions are implemented.

**Discussion of examples**

There are several things to be learned from the plug flow example:

1. The example shows the effect of using central differences for the convection term in convection-diffusion equations (not advisable when convection dominates conduction/diffusion).

2. The example contains the case of pure conduction (heat conduction in a slab) as a special case when $Pe = 0$ and $\beta = 1/2$. This is when the largest time constants occur.

3. The example provides an analogy for both example 1 (composition dynamics of stripping column) and example 2 (pressure dynamics of a train of vessels).

   For stripping columns, the largest time constant occurs when the operating line and the equilibrium line are parallel. The phenomenon may then be interpreted as caused by diffusion like—or random

walk—behavior. In practice, the equilibrium line and the operating line are not parallel, and the column then behaves much more like plug flow, with short time constants.

The second example, pressure dynamics in a train of vessels, is seen to be analoguous to pure heat conduction in a slab. It is important to note, however, the assumption of negligible inertia effects of the gas.

So far, the focus has been on transfer functions. For insight/visualization, it may be useful to use the different physical systems as analogies for each other. We will do this for binary distillation.

# 3 Analyzing binary distillation

Above, we have presented various cascade systems, which all turns out to have the same mathematical structure. We therefore have a rich source of analogies, which we can use when analyzing cascade processes. In this section, we use the plug flow analogy to shed some light on the dynamics of binary distillation columns. However, we first present some numerical observations regarding the relation between the slow time constant and the number of stages of a binary distillation column. We investigate the effect of the reflux from the condenser and the reboiler, as well as the effect of the vapor-liquid equilibrium.

We start with a simple distillation model.

## 3.1 A simple distillation model

We present a simple model for the concentration dynamics of a binary distillation column, which serves as the starting point for the numerical observations presented in the next subsection. The column is depicted in Fig. 5a.

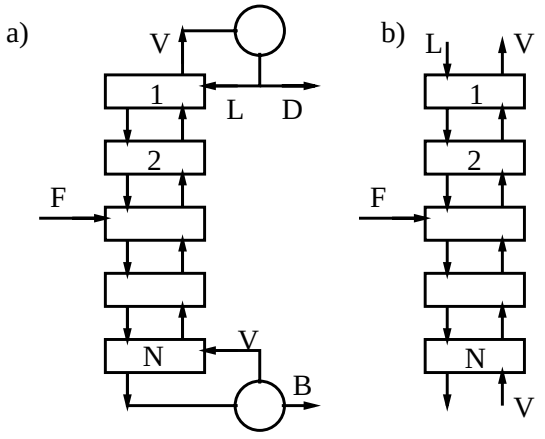


Figure 5: Binary distillation column (a) and a modified open end version (b).

### Mathematical model

As a model for the column, we take (mass balance for light component at stage $j$):

$$M\frac{dx_j}{dt} = L(x_{j-1}-x_j)+V(y_{j+1}-y_j); \quad y_j = \frac{\alpha x_j}{1+(\alpha-1)x_j} \tag{27}$$

where the notation is similar to the stripping column presented earlier.

This equation may be linearized around the steady state to get :

$$M\dot{x}_j = Lx_{j-1} - (L+VK_j)x_j + VK_{j+1}x_{j+1} \tag{28}$$

where $x$ is now a deviation variable. The slope of the equilibrium line, $K_j$, is given by $K_j = \frac{dy_j}{dx_j} = \frac{\alpha}{[1+(\alpha-1)x_j]^2}$.

## 3.2 Numerical observations

We now present some numerical observations regarding the slow time constant of the column. The starting point—the base case—is the column model described above. We then do various modifications in order to test the sensitivity of the results to some of the assumptions.

### Assumptions

The following assumptions and parameter values are used in the computations:

1. Constant relative volatility, $\alpha = 1.5$
2. Constant molar holdup, $M = 1$, on each stage;
3. Constant molar flows, $L = 2.635$, $V = 3.135$, and distillate flow rate $D = 0.5$;
4. Feed flow rate and mole fraction at the middle of the column, $F = 1$ and $z = 0.5$;
5. Total condenser (holdup $M = 1$); and
6. Reboiler as one equilibrium stage.

### Cases studied

We compare the following cases:

- **Base case.** This is the real column model described above.
- **Case 1.** As the base case, but with the equilibrium line approximated by two straight segments, as shown in Fig. 6. The slopes of the segments are $\alpha$ and $1/\alpha$, where $\alpha = 1.5$ is the relative volatility. Thus, this is an approximation to the equilibrium line for high and low values of $x$—the mole fraction of light component.

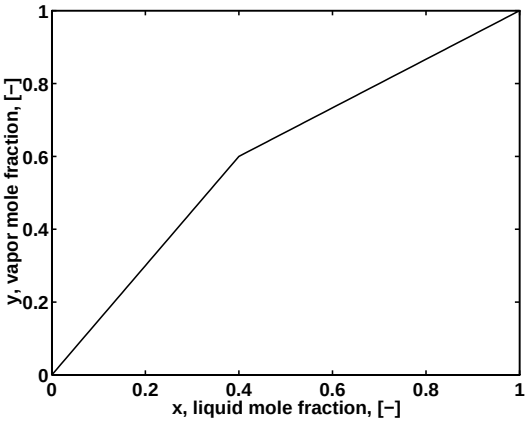


Figure 6: Simplified vapor-liquid equilibrium, consisting of two linear segments

- **Case 2.** As the base case, but with the reboiler and condenser removed, as shown in Fig. 5b. Instead, there is a feed, $L$, of pure light component at the top of the column, and a feed, $V$, of pure heavy component at the bottom. The purpose of the arrangement is to see the effect of the reflux from the reboiler and the condenser; one would, of course, never build such an arrangement.
- **Case 3.** As case 2, but with **impure** feeds $L$ and $V$. The impurities are $x = 0.95$ at the top and $y = 0.05$ at the bottom.

**The slow time constant**

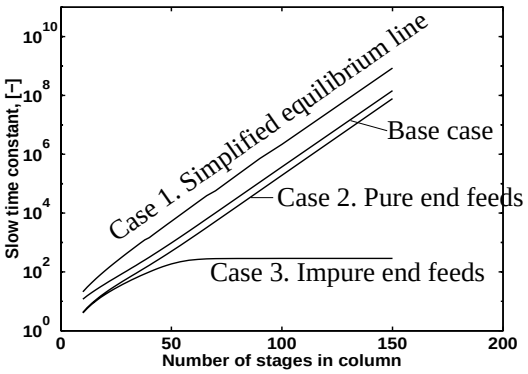


Figure 7: Slow time constant as a function of number of stages

Figure 7 shows the dependence of the slow time constant (resiprocal of the smallest eigenvalue) as a function of the number of stages in the column—all other parameters kept constant. As can be seen, for all cases except case 3, the results are straight lines in a semi-logarithmic plot, which means that the time constant increases **exponentially** with the number of stages in the column. For case 3—impure feeds $L$ and $V$ at the top and bottom—the time constant approaches a limit as $N \to \infty$.

### 3.3 Conceptual models for binary distillation

The purpose of this subsection is to shed some light on the observations above.

In the stripping column example earlier, it was shown that the time constant may be proportional to $N^2$—the square of the number of stages—when the equilibrium line and the operating line are parallel, and slower when they are not parallel. However, this is only the case when both ends of the column are open. In fact, in the numerical case study of binary distillation above, we found that the time constant may increase **exponentially** with the number of stages when two such linear cascades are interconnected (Case 1 above), and that this behavior is qualitatively similar to the behavior of binary distillation with constant relative volatility (The base case).

We start by describing a very simple model—an analogy—which exhibits a dynamic behavior similar to a binary distillation column. The relation between this simple model and the binary distillation column is presented afterwards.

Similar analogies have been presented previously, e.g. Rosenbrock, 1962.

**An analogy for a binary distillation column**

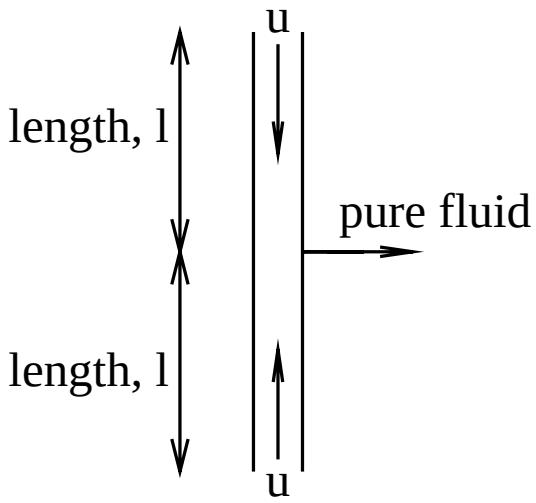


Figure 8: Pipe and tank analogy to binary distillation

Consider the system shown in Fig. 8, showing a pipe of length $2l$, initially containing a fluid with an impurity (concentration $x$). Pure fluid enters at both ends of the pipe, and flows towards the middle of the pipe, where pure fluid is removed. That is, the outlet at the middle of the pipe does not let the impurity through. This means

that the only way the impurity may leave the pipe, is by diffusing through the pipes against the flowing current. As a model of this convection-diffusion process, we take:

$$\frac{\partial x}{\partial t} + \frac{\partial (ux)}{\partial z} = \frac{\partial}{\partial z}(\nu \frac{\partial x}{\partial z}) \tag{29}$$

where $x$ is the concentration of impurity, $u$ and $\nu$ are the fluid velocity and the diffusivity, and $z$ is the position in the pipe.

It is shown in Appendix C that the slowest time constant of this system may be approximated as :

$$\tau \approx \frac{\nu}{u^2} e^{\frac{ul}{\nu}}; \quad for \quad \frac{ul}{\nu} >> 1 \tag{30}$$

Hence, the time constant for depletion of impurity increases **exponentially** with the length of the pipe. This exponential dependence may not come as a surprise, since countercurrent diffusion is not very effective; and the pipe therefore retains the impurity quite effectively.

Note for later use that equation 29 may be approximated by the finite difference equation:

$$\frac{dx_i}{dt} + (\frac{u_i}{\Delta z} x_i - \frac{u_{i-1}}{\Delta z} x_{i-1}) = \frac{\nu_i}{\Delta z^2}(x_{i+1} - x_i) - \frac{\nu_{i-1}}{\Delta z^2}(x_i - x_{i-1}) \tag{31}$$

### The binary distillation model

We now proceed with the model for binary distillation. The overall aim is to make a comparison between the column model and the conceptual pipe model.

Consider the linearized model of the binary distillation column analyzed in the previous section, where x is the mole fraction of light component—or more correctly, the deviation of that mole fraction from steady state:

$$M\dot{x}_j = Lx_{j-1} - (L + VK_j)x_j + VK_{j+1}x_{j+1} \tag{32}$$

This may be rewritten as:

$$\dot{x} + (u_j x_j - u_{j-1} x_{j-1}) = \nu_j (x_{j+1} - x_j) - \nu_{j-1}(x_j - x_{j-1}) \tag{33}$$

where the equivalent velocity and diffusivity are expressed as:

$$u_j \equiv \frac{L - VK_{j+1}}{M}; \quad \nu_j = \frac{VK_{j+1}}{M} \tag{34}$$

Thus, the distillation model, eq. 33, is seen to be a **finite difference** analog to the pipe model, eq. 29. Hence, we expect their behavior to be very similar.

Thus, we may see the analogy to the pipe model:

1. First, note that the deviation variable, $x$—which is the deviation of the mole fraction from steady state—is a **conserved quantity**, as defined by eq. 8, $a_{j+1} + b_j + c_{j-1} = 0$. Indeed, from the linearized distillation model, eq. 32, we get: $a_{j+1} + b_j + c_{j-1} = [L] + [-(L + VK_j)] + [VK_j] \equiv 0$.

   What this conservative property means, is that an increase in $x$ at one stage corresponds to a decrease in a neighboring stage; i.e. the deviation in mole fraction from steady state can not "vanish" inside the column, but has to "leave" through the column ends. This is similar to the case of the impurity in the pipe analogy, which also has to leave through the ends.

   That the deviation, $x$, from steady state operation, represents some sort of "conserved" property, has also been noticed by Rosenbrock, 1960.

2. The "velocity" $u_j \equiv \frac{L - VK_{j+1}}{M}$ is directed from the ends of the column towards the middle of the column. This follows from the fact that the slope of the equilibrium line, $K_{j+1}$, is larger than the slope of the operating line, $L/V$, at the bottom of the column, and smaller at the top of the column. Hence, this velocity, $u$, corresponds to the velocity in the two pipes in the simple model.

3. The effective diffusivity in the distillation column is $\nu_j = \frac{VK_{j+1}}{M}$.

4. The pipe lengths, $2l$, in the simple model corresponds to the number of stages in the distillation column.

5. The deviation variable tends to accumulate at points where the equilibrium- and operating lines are parallel, i.e. where $u_j = \frac{L - VK_{j+1}}{M} = 0$.

6. As with the pipe model, the numerical observations presented earlier indicate that distillation time constants increase exponentially with the number of stages when $N \to \infty$ (when all flow rates are kept constant).

### Definitions

For subsequent discussion, we define some concepts:

- **Equivalent velocity**. $u_j \equiv \frac{L - VK_{j+1}}{M}$
- **Equivalent diffusivity**. $\nu_j = \frac{VK_{j+1}}{M}$.
- **Stationary point**. A point in the column—i.e. a stage—where the equivalent velocity $u_j$ is zero. This corresponds to parallel equilibrium and operating lines.
- **Accumulation points**. A stationary point where the equivalent velocities on each side are pointing **towards** the stationary point—not **from** the stationary point. The reason for the term "accumulation point" is that the deviation variable, $x$, tends to "flow" towards it, which means that it tends to accumulate at such points.

### A numerical experiment

In order to illustrate the relation between the distillation column and the pipe analogy, consider the following thought experiment: Assume that we inject some extra light component into tray 20 (counted from the top of the column) at time $t = 0$ in a column with 82 stages—the base case above. This corresponds to an impulse response with input at tray 20.

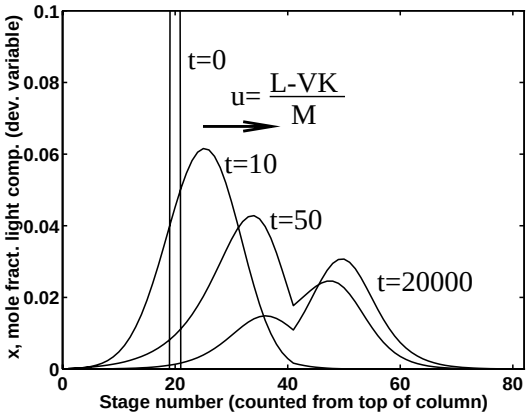


Figure 9: Impulse in light component at stage 20.

**Remark:** The reason for showing a case where the injection of extra light component is at tray 20—and not, for example, the feed tray, which would be more realistic in practice—is that it makes it easier to see the nature of the column behavior. In particular, it makes it easier to see the effect of the equivalent velocity, which is rather small near the feed tray.

Fig. 9 shows the resulting column concentration profiles (deviation variable) through the column for different times. As can be seen, the excess amount of light component is first located at tray 20. It then moves towards the center of the column with velocity $u_j \approx \frac{L-VK_{j+1}}{M}$, spreading according to a diffusivity $\nu_j \approx \frac{VK_{j+1}}{M}$. In the long run, it tends to accumulate at tray 35 and 49—the accumulation points—where the operating- and equilibrium lines are approximately parallel, i.e. where the velocity is zero, $u_j \approx \frac{L-VK_{j+1}}{M} = 0$. The concentration profile relatively quickly assumes the shape of the slow eigenvector of the linearized system, and then vanishes very slowly, keeping the shape of the slow eigenvector as it vanishes.

That the operating- and equilibrium lines are parallel at the accumulation points–stage 35 and 49–may be seen in the McCabe-Thiele diagram shown in Fig. 10.

Fig 11 shows the **equivalent velocity profile** in the column ($u_j = \frac{L-VK_{j+1}}{M}$). As can be seen, there are three stationary points ($u = 0$), of which stage 35 and 49 are accumulation points. Note that there is a region, between stage 35 and 49, where the "flow" is **outwards** from the feed tray towards the column ends. In the rest of the

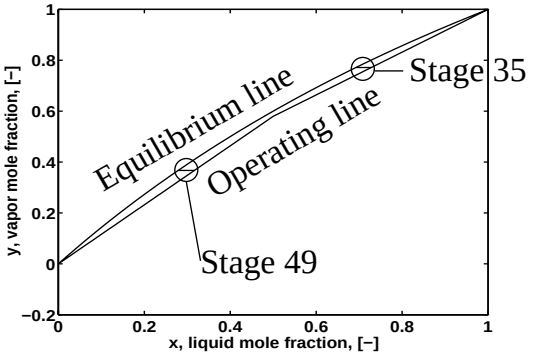


Figure 10: McCabe-Thiele diagram. Accumulation points, stage 35 and stage 49 are shown

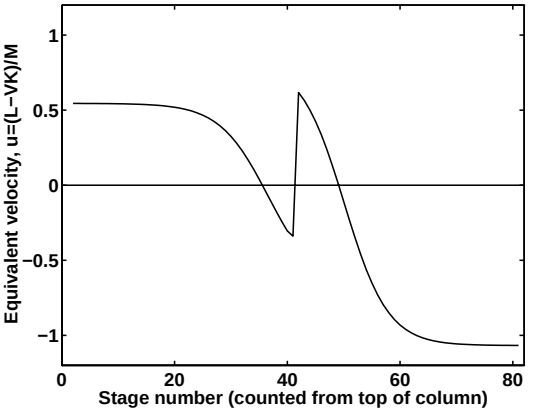


Figure 11: Velocity profile in column

column the "flow" is from the ends towards the feed tray.

This sheds some light on the dynamic behavior of the binary distillation column. However, we have not explained why the open ended column with impure feeds at the column ends—case 3 above—has a time constant that approaches a fixed value as $N \to \infty$ rather than increasing exponentially as was the case for the other cases.

**Open ended column with impure feeds**

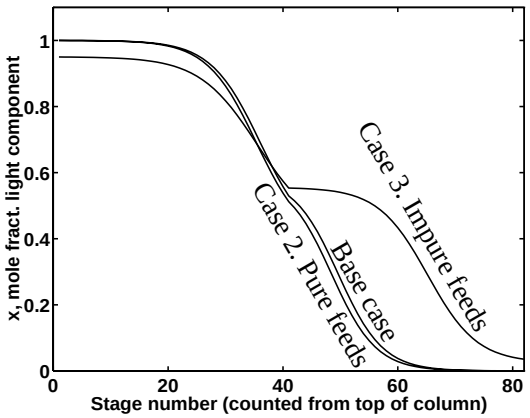


Figure 12: Comparison of concentration profiles

Figure 12 compares concentration profiles (absolute values, not deviation variables) through the column for the base case, case 2 (open ends, pure feeds) and case 3 (open ends, impure feeds). It can be seen that the concentration profiles are similar, except that in case 3 (impure feeds), there is a flat region below the feed tray. The current plot applies to impurities $x = 0.95$ at the top and $y = 0.05$ at the bottom of the column. Similar flat concentration profiles are obtained with other values of the impurities; however, sometimes the flat region close to the feed tray is at the **upper** side of the feed tray.

This flat region in case 3 implies that one of the accumulation points stays close to the column end as we increase the number of stages. In fact, the distance between the accumulation point and the column end approaches a fixed value as the total number of stages is increased. This distance corresponds to the equivalent length of pipe in the pipe-and-tank analogy; thus, the corresponding time constant approaches a fixed value as $N \to \infty$.

**Steady state sensitivity**

To complete the numerical experiment, we show that the steady state sensitivity of the column is also very high. Fig. 13 shows the concentration profile of light component in the column (absolute value, not deviation variable) for three different values of $z$—the mole fraction of light component in the feed. As can be seen, very small

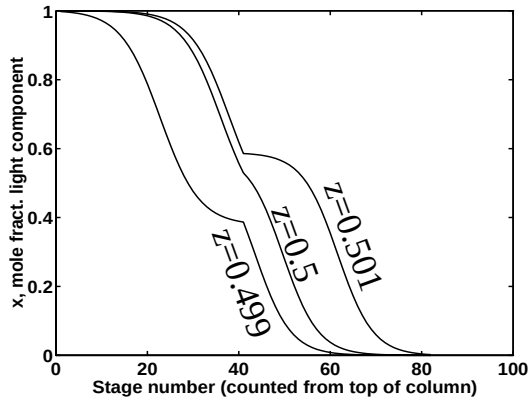


Figure 13: Sensitivity of concentration profiles

changes in $z$ leads to very large changes in the concentration profile. The changes are largest near tray 35 and 49—the accumulation points.

## 4 Discussion

**Relation to a state space point of view**

Above, we have examined cascade systems with one very small eigenvalue, which results in very large time constants. In this subsection, we discuss this in relation to a state space point of view, and try to make a connection between steady state sensitivity and the dynamic behavior of such systems. We argue that the dynamic behavior of the system is essentially one-dimensional.

In order to formulate the argument, we define the gain of a matrix, say $G$, in the input direction $u$ to be: $gain = \frac{||Gu||}{||u||}$. In this expression, we define the direction of $u$ to be an input direction, and the direction of $Gu$ to be the corresponding output direction. In this sense, we talk of gains and directions for any matrix–not only transfer functions.

Consider a stable system described by a state space model on the form:

$$\dot{x} = Ax + Bu \tag{35}$$

We assume that the $A$-matrix has one real Left Half Plane eigenvalue very close to zero; the other eigenvalues are much faster. Note that this is the case for the interconnected cascades described in this paper; these have one very long time constant, the others are fast.

From the definition of the slow eigenvalue, $\lambda_{slow}$, we get:

$$Ax_{slow} = \lambda_{slow} x_{slow} = very \quad small \tag{36}$$

which means that the gain of $A$ is very small in the input direction corresponding to the slow eigenvector, $x_{slow}$. Turning things around, this implies that the gain of **the inverse**, $A^{-1}$, is very **large** in the **output** direction corresponding to the direction of the slow eigenvector. Since

the steady state gain of **the system** is given by

$$x = -A^{-1}B \cdot u \tag{37}$$

this implies that small changes in the inputs, $u$, will typically cause large changes in the states, $x$, in the direction of the slow eigenvector. Hence, the steady state gain is typically very much aligned with the slow dynamics. In other words, the dynamics is essentially **one-dimensional**; that is, the state tends to stay on a line $x = p \cdot x_{slow}$, where $p$ is a scalar parameter. However, exceptions may occur if a weak output directions of the $B$-matrix is aligned with the weak output directions of the $A$-matrix, in which case the situation may be different.

One might conjecture that this one-dimensional behavior exist also in the non-linear case, that is, for large inputs, $u$, in the nonlinear cascade models. Locally–that is, reasonably close to steady state–one would expect the slow eigenvector of the linearized system to be the tangent of a one-dimensional slow manifold, say $x = x(p)$, where $p$ is a scalar parameter. The state, $x$, would then tend to stay on this slow manifold under varying inputs, resulting in essentially one-dimensional behavior.

### "All trays have the same response"

Having realized that one mode is slow, Skogestad and Morari (1987) derived very accurate formulaes for the slow time constant of binary distillation columns, based on the assumption that all trays in a column have the same response. That is, they assumed that the change in mole fraction of light component at tray $j$ may be expressed as $\Delta x_j(t) = a_j f(t)$, where $a_j$ represents the amplitude at tray $j$ and $f(t)$ is the response–the same for all stages.

In essence, this is an assumption of one-dimensional (linear) behavior. In the light of the previous subsection, the good results obtained by Skogestad and Morari may therefore not come as a great surprise.

## 5 Conclusion

In this paper, we have shown how simple cascade systems may be analyzed; first by showing how the poles of scalar cascades may be determined from the subsystems transfer functions. Knowing the pole locations, it is then straightforward to find, for example, time responses of such systems.

Application of the results to stripping or adsorbtion columns with linear equilibrium lines, show that the slowest time constant of these columns approach a fixed value when the number of stages becomes large, i.e. when $N \to \infty$ (equation 14). An exception occurs when the equilibrium- and the operating lines are parallel, in which case the slowest time constant increases as $N^2$—the square of the number of stages.

We then showed that the interconnection of scalar cascades may result in very long time constants, and that this may be thought of as an effect of **positive feedback** between the cascades. A distillation column may be thought of as such an interconnection of two cascades. In fact, the slow time constant of binary distillation increases exponentially with the number of stages when all other quantities are kept constant.

Using a plug flow analogy, we then made an analysis of a specific case—binary distillation. By numerical experiments on such a system, we illustrated the dynamic behavior. The concentration dynamics of the column resembles the behavior of plug flow with diffusion, which is not surprizing since the component mass balance of the column may be thought of as a finite difference analog of the mass balance of the plug flow partial differential equation.

### Notation

| | |
|---|---|
| $a$ | coefficient in eq. 7 |
| $b$ | coefficient in eq. 7 |
| $c$ | coefficient in eq. 7 |
| $D$ | distillate flow rate |
| $F$ | feed flow rate |
| $g(s)$ | transfer function in scalar cascade (eq. 4) |
| $G(s)$ | transfer function in multivariable cascade (eq. 1) |
| $h$ | discretization length in eq. 24 |
| $h(s)$ | transfer function in scalar cascade (eq. 4) |
| $H(s)$ | transfer function in multivariable cascade (eq. 1) |
| $k_n$ | factor defined by eq. 6 |
| $K$ | slope of vapor-liquid equilibrium line |
| $L$ | liquid molar flow rate |
| $L(s) = G(s)H(s)$ | "loop" transfer function in cascade |
| $M$ | molar holdup on tray |
| $N$ | number of trays in column |
| $\mathcal{N}$ | nonlinear operator |
| $p$ | pressure (deviation variable) |
| $P$ | absolute pressure |
| $Pe = \frac{uh}{\nu}$ | peclet number |
| $s$ | Laplace variable |
| $S(s)$ | transfer function between two consecutive stages |
| $t$ | time |
| $T$ | temperature |
| $T(s)$ | overall transfer function for cascade |
| $u$ | equivalent velocity |
| $V$ | vapor molar flow rate |
| $x$ | liquid mole fraction of light component |
| $y$ | vapor mole fraction of light component |
| $z$ | space coordinate; or feed mole |

| | |
|---|---|
| | fraction of light component |

Greek

| | |
|---|---|
| $\alpha$ | constant relative volatility |
| $\beta$ | Parameter in eq. 10 |
| $\phi$ | flux of chemical species |
| $\nu$ | diffusivity |
| $\tau$ | time constant |

Subscripts

| | |
|---|---|
| $i$ | index over stages in column |
| $j$ | index over stages in column |
| $N$ | last stage in column |

## References


[1] Celebi, C and E.H. Chimowitz, 1985. Analytic Reduced-Order Dynamic Models for Large Equilibrium Staged Cascades. AIChE J., 31, 12, pp. 2039-2051

[2] Cho, Y.S and B. Joseph, 1983. Reduced-Order Steady State and Dynamic Models for Separation Processes. AIChE J., 29, 2, p. 261-276

[3] Croockewit, P., C. C. Honig and H. Cramers, 1955. Chem Eng Sci, 1955, 4, p 111

[4] Fuentes, C. and W.L. Luyben, 1983. Control of High-Purity Distillation Columns. Ind. Eng. Chem. Proc. Des. Dev., 22, pp. 361-366

[5] Haagensen, A.J and F.P. Lees, 1966. The Frequency Response of a Plate Gas Absorbtion Column. Chem. Eng. Sci., 21, pp. 77-86

[6] Hwang,Y.L., 1990. Dynamics of continuous countercurrent mass-transfer processes - IV. Multicomponent waves and assymetric dynamics.Chem. Eng. Sci., 45, pp. 2907-2915

[7] Hwang,Y.L., 1991. Nonlinear Wave Theory for Dynamics of Binary Distillation Columns. AIChE J. 37, pp. 705-723

[8] Kapoor, N. and T.J. McAvoy, 1986a. An Analytical Approach to Approximate Dynamic Modeling of Distillation Towers. Ind. Eng. Chem. Res., 26, 12, pp. 2473-2482.

[9] Kapoor, N. and T.J. McAvoy, 1986b. Effect of Recycle Structure on Distillation Tower Time Constants. AIChE J., 32, 3, pp. 411-418

[10] Kienle A. and W. Marquardt, 1992. Nonlinear Waves in Counter-Current Separation Processes Involving Highly Nonideal Multicomponent Mixtures. AIChE J., 1992

[11] Kim, C. and J.C. Friedly, 1974. Approximate Dynamic Modeling of Large Staged Systems. Ind. Eng. Chem. Proc. Des. Dev., 13, 2, pp. 177-181

[12] Lapidus, L. and N.R. Amundson, 1950. Ind. Eng. Chem., 42, p. 1071

[13] Levy, R.E., A.S. Foss and E.A. Grens, 1969. Response Modes of a Binary Distillation Column. IEC Fund., 8, 4, pp. 765-776

[14] Marquardt, W., 1990. Traveling waves in chemical processes. Ind.Chem.Eng., 30, pp. 585-606

[15] Montroll, E.W and G.F. Newell, 1952. Unsteady-State Separation Performance of Cascades. J. of Appl. Physics, 23, 2, pp. 184-194

[16] Osborne, A., 1971. The calculation of Unsteady State Multi-component Distillation Using Partial Differential Equations. AIChE J., 17, 3, pp. 696-703

[17] Rademaker, O., J. E. Rijnsdorp and A. Maarleveld, 1975. Dynamics and Control of Continuous Distillation Units. Elsevier, Amsterdam, 1975

[18] Rosenbrock, H.H., 1960. A Theorem of "Dynamic Conservation" for Distillation Columns. Trans. Instn. Chem. Engrs. 38, pp. 279-287

[19] Rosenbrock, H.H., 1962. The Transient Behavior of Distillation Columns and Heat Exchangers. A Historical and Critical Review. Trans. Instn. Chem. Engrs. 40, pp. 376-384

[20] Skogestad, S. and M. Morari, 1987. The Dominant Time Constant for Distillation Columns. Comput. Chem. Engng., 11, 6, pp. 607-617

[21] Tabrizi, M.H.N., 1990. An investigation into the dynamics of the distillation column, Search for a wave effect. IEEE Proc., pp. 599- 602

[22] Williams, T.J., 1963. The Status of Studies of the Dynamics of Mass-transfer Operations—A review and Commentary. Chem. Eng. Progr. Symp. Ser. 59, 46, pp. 1-8.

[23] Wong, K.T. and R. Luus, 1980. Model Reduction of High-Order Multistage Systems by the Method of Orthogonal Collocation. The Canadian J. of Chem. Eng., 58, pp. 382-388

[24] Wong, S.K.P. and D.E. Seborg, 1986. Low-order Nonlinear, Dynamic Models for Distillation Columns. Proceedings ACC 86, Seattle.

## Appendix A. Derivation of $T_N$

We are deriving equation 5, i.e.:

$$T_N = \frac{g(s)^N}{\Pi_n(1 - k_n g(s)h(s))} \tag{38}$$

Consider the transfer function $S_j$ from eq. 3,

$$S_j = (1 - hS_{j-1})^{-1} g \tag{39}$$

First pull out a factor $g$ to get a transfer function $R_j$, i.e. $S_j = R_j g$. The recursion then becomes:

$$R_j = \frac{1}{1 - L \cdot R_{j-1}}; \quad L \equiv gh \tag{40}$$

Decomposing $R_j$ into its nominator and denominator polynomial (in $L$, not in $s$!), yields:

$$\frac{n_j(L)}{d_j(L)} = \frac{d_{j-1}(L)}{d_{j-1}(L) - L n_{j-1}(L)} \tag{41}$$

from which we obtain recursion formulas for $n_j$ and $d_j$ (dropping the $L$-argument for convenience):

$$n_j = d_{j-1} \tag{42}$$

$$d_j = d_{j-1} - L n_{j-1} = d_{j-1} - L d_{j-2} \tag{43}$$

The last equation is a homogeneous linear difference equation with constant coefficients. Its characteristic equation is:

$$\lambda^2 = \lambda - L \tag{44}$$

with roots:

$$\lambda_{1,2} = \frac{1 \pm \sqrt{1 - 4L}}{2} \tag{45}$$

The general solution is then on the form

$$d_j = C_1 \lambda_1^j + C_2 \lambda_2^j, \quad d_0 = d_1 = 1 \tag{46}$$

Eliminating $C_1$ and $C_2$ using the boundary conditions ($d_0 = d_1 = 0$) yields:

$$d_j = \frac{\lambda_1^{j+1} - \lambda_2^{j+1}}{\lambda_1 - \lambda_2} \tag{47}$$

In order to obtain eq. 38, we have to factorize this polynomial, i.e. we have to find the roots of $d_j(L) = 0$:

$$\frac{\lambda_1^{j+1} - \lambda_2^{j+1}}{\lambda_1 - \lambda_2} = 0 \quad \Rightarrow \quad \frac{(\frac{\lambda_1}{\lambda_2})^{j+1} - 1}{\frac{\lambda_1}{\lambda_2} - 1} = 0 \tag{48}$$

Solving for $\frac{\lambda_1}{\lambda_2}$ (roots of unity):

$$\frac{\lambda_1}{\lambda_2} = e^{\frac{2\pi k}{j+1}}, \quad k = 1, 2 \cdots j \tag{49}$$

Substituting for $\frac{\lambda_1}{\lambda_2}$ using eq. 44, and solving for $L \equiv gh$:

$$L_k = \frac{1}{4\cos^2(\frac{k\pi}{j+1})}, \quad k = 1, 2, \cdots j \tag{50}$$

Noting that this expression counts the roots twice, we may now factorize $d_j$:

$$d_j = \Pi_{k=1}^{\lfloor \frac{j+1}{2} \rfloor} (1 - \frac{L}{L_k}), \quad L \equiv gh \tag{51}$$

Finally, we may find $T_N$:

$$\begin{aligned} T_N &= \Pi_{j=1}^N S_j = \Pi_{j=1}^N R_j g = \Pi_{j=1}^N \frac{n_j}{d_j} g \\ &= g^N \Pi_{j=1}^N \frac{d_{j-1}}{d_j} = \frac{g^N}{d_N} \\ &= \frac{g(s)^N}{\Pi_n(1 - k_n g(s)h(s))} \end{aligned} \tag{52}$$

where:

$$k_n = 1/L_n = 4\cos^2(\frac{n\pi}{N+1}), \quad n = 1, 2, \cdots \lfloor \frac{N+1}{2} \rfloor \tag{53}$$

## Appendix B. Dynamics of a train of vessels

The model for the train of vessels are described by a mass balance, a flow relation, and a polytropic relation for each volume $j$, $j = 1, 2, \cdots N$:

$$\begin{aligned} \frac{d}{dt}(\bar{\rho}_j V) &= F_{j-1} - F_j \\ F_j = C\sqrt{\Delta p}, \quad \Delta p &\equiv p_j - p_{j+1} \\ p &= k\bar{\rho}^n \end{aligned} \tag{54}$$

where $F_j$ and $\bar{\rho}_j$ are molar flow and density; $V$ and $p$ are the volume of a vessel and its pressure; and $n$ is a polytropic coefficient ($n = 1$ for isothermal vessels; $n = \gamma \equiv$ *adiabatic constant* for isentropic vessels; in general $1 < n < \gamma$). It is implicitly assumed that inertia effects are unimportant, and that the pressure drops and flows are more or less the same between all vessels.

These equations may be linearized to get:

$$\begin{aligned} V\frac{d\delta\rho_j}{dt} &= \delta F_{j-1} - \delta F_j \\ \delta F_j = \frac{C}{2\sqrt{\Delta p}}(\delta p_j - \delta p_{j+1}) &= \frac{F_j}{2\Delta p}(\delta p_j - \delta p_{j+1}) \\ \delta p = kn\bar{\rho}^{n-1}\delta\bar{\rho} &= \frac{np}{\bar{\rho}}\delta\bar{\rho} \end{aligned} \tag{55}$$

and combined to one equation in $\delta p$:

$$2\tau\delta\dot{p}_j = \delta p_{j+1} - 2\delta p_j + \delta p_{j-1} \tag{56}$$

where $\tau = \frac{\Delta p \bar{\rho} V}{F_j np} = \frac{\Delta p}{np}\tau_{res}$ is the time constant of a single vessel, and $\tau_{res} = \frac{\bar{\rho}V}{F_j}$ is the residence time of one vessel.

## Appendix C. Slow time constant of pipe analogy for distillation

We are deriving the expression for the slow time constant for the pipe analogy in section 3.3:

$$\tau \approx \frac{\nu e^{\frac{ul}{\nu}}}{u^2} \quad when \quad \frac{ul}{\nu} >> 1 \tag{57}$$

The pipe system is shown in Fig. 8. We consider only half of the pipe, $z \in [0, l]$, since the system is symmetric about $z = l$.

The starting point for the derivation is the mass balance equation for the impurity, $x$:

$$\frac{\partial x}{\partial t} + u\frac{\partial x}{\partial z} = \nu\frac{\partial^2 x}{\partial z^2} \tag{58}$$

with boundary conditions:

$$x(0) = 0 \quad and \quad \phi(l) = [ux - \nu\frac{\partial x}{\partial z}]_{z=l} = 0 \tag{59}$$

The first of these boundary conditions states that there is pure fluid at the inlet of the pipe; the other that the flux, $\phi$, of impurity across the middle of the pipe ($z = l$) is zero.

To find the slow eigenvalue, we take the Laplace transform of the mass balance, eq. 57:

$$\nu x'' - ux' - sx = 0 \tag{60}$$

where $s$ is the Laplace variable. The general solution of this equation is on the form:

$$x = Ae^{\lambda_1 z} + Be^{\lambda_2 z} \tag{61}$$

where the parameters are still to be determined.

Substituting this solution into the boundary conditions yields:

$$x(0) = 0 \Rightarrow \qquad A + B = 0 \tag{62}$$

$$\phi(l) = [ux - \nu\frac{\partial x}{\partial z}]_{z=l} = 0 \Rightarrow \quad A(u - \nu\lambda_1)e^{\lambda_1 l} + B(u - \nu\lambda_2)e^{\lambda_2 l} = 0 \tag{63}$$

These two equation for the boundary conditions may be put in matrix form as:

$$\begin{pmatrix} (u - \nu\lambda_1)e^{\lambda_1 l} & (u - \nu\lambda_2)e^{\lambda_2 l} \\ 1 & 1 \end{pmatrix} \begin{pmatrix} A \\ B \end{pmatrix} = 0 \tag{64}$$

For this matrix equation to have non-trivial solutions, the determinant of the matrix has to be zero:

$$\begin{aligned} 0 &= det \begin{pmatrix} (u - \nu\lambda_1)e^{\lambda_1 l} & (u - \nu\lambda_2)e^{\lambda_2 l} \\ 1 & 1 \end{pmatrix} \\ &= (u - \nu\lambda_1)e^{\lambda_1 l} - (u - \nu\lambda_2)e^{\lambda_2 l} \end{aligned} \tag{65}$$

which may be written (divide by $e^{\lambda_2 l}$):

$$(u - \nu\lambda_1)e^{(\lambda_1 - \lambda_2)l} - (u - \nu\lambda_2) = 0 \tag{66}$$

Solving this equation for the pole, $s$, closest to zero, yields the desired result. However, we must first find approximations for the terms in this equation. First, the $\lambda' s$ are given by the characteristic equation:

$$\nu\lambda^2 - u\lambda - s = 0 \tag{67}$$

which yields:

$$\lambda_1 = \frac{u + \sqrt{u^2 + 4\nu s}}{2\nu} \quad \lambda_2 = \frac{u - \sqrt{u^2 + 4\nu s}}{2\nu} \tag{68}$$

from which we may find the following approximations for small $s$ (Taylor series around $s = 0$):

$$u - \nu\lambda_1 \approx -\frac{s\nu}{u} \quad u - \nu\lambda_2 \approx u + \frac{s\nu}{u} \tag{69}$$

Moreover, we may find the following approximation (Taylor series):

$$e^{(\lambda_1 - \lambda_2)l} = e^{\frac{\sqrt{u^2 + 4\nu s}}{\nu} l} \approx e^{\frac{ul}{\nu}}(1 + \frac{2sl}{u}) \tag{70}$$

Inserting this into eq. 65, neglecting second order terms in $s$ and solving for $s$, yields:

$$s = -\frac{u^2}{\nu(1 + e^{\frac{ul}{\nu}})} \tag{71}$$

from which the desired formula for the slow time constant may be found:

$$\tau = -1/s = \frac{\nu}{u^2}(1 + e^{\frac{ul}{\nu}}) \approx \frac{\nu}{u^2}e^{\frac{ul}{\nu}}; \quad for \quad \frac{ul}{\nu} >> 1 \tag{72}$$

Thus, we have found the approximation for $\tau$.

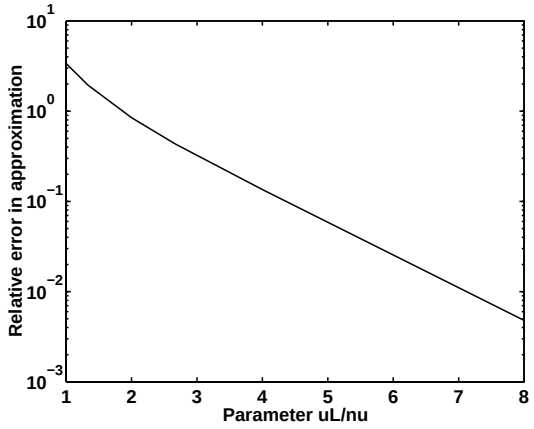


Figure 14: Relative error in the approximate formula, eq. 71, as function of $\frac{ul}{\nu}$

In order to check how large $\frac{ul}{\nu}$ has to be for this approximation to be valid, we calculated the relative error in $\tau$ as a function of $ul/\nu$, using MATLAB (i.e. numerically). The resulting plot is shown in Fig. 71. As can be seen, the relative error is less than about 10% for $ul/\nu > 4$ and less than about 1% for $ul/\nu > 7$.